Non-linear online low-frequency EEG decoding of arm movements during a pursuit tracking task

Víctor Martínez-Cagigal, Reinmar J. Kobler, Valeria Mondini, Roberto Hornero, *Senior Member, IEEE*, and Gernot R. Müller-Putz, *Member, IEEE*

***Abstract*— Decoding upper-limb movements in invasive recordings has become a reality, but neural tuning in non-invasive low-frequency recordings is still under discussion. Recent studies managed to decode movement positions and velocities using linear decoders, even developing an online system. The decoded signals, however, exhibited smaller amplitudes than actual movements, affecting feedback and user experience. Recently, we showed that a non-linear offline decoder can combine directional (e.g., velocity) and non-directional (e.g., speed) information. In this study, it is assessed if the non-linear decoder can be used online to provide real-time feedback. Five healthy subjects were asked to track a moving target by controlling a robotic arm. Initially, the robot was controlled by their right hand; then, the control was gradually switched until it was entirely controlled by the electroencephalogram (EEG). Correlations between actual and decoded movements were generally above chance level. Results suggest that information about speed was also encoded in the EEG, demonstrating that the proposed non-linear decoder is suitable for decoding real-time arm movements.**

I. Introduction

Current brain–computer interface (BCI) research is gently moving from decoding categorical classes that represent certain actions (e.g., through motor imagery) toward decoding continuous users' movements [1]. In this sense, imagined upper-limb movements were successfully decoded via invasive recordings [2]; however, the usability of non-invasive methods such as EEG for the same purpose is still under discussion [3–7].

Previous studies demonstrated that kinematic information of executed [3], [6], observed [6], [8] and imagined [5] upper-limb movements is encoded in the low-frequency EEG band, making it possible to decode positions and velocities using linear algorithms, such as partial least squares (PLS) regression [5], [6] or Kalman filters [8–10]. First offline studies assessed whether neural tuning can be retrieved from EEG [3], [5] and studied the locations of the cortical sources [6]. A step further was performed in [10] to develop an online decoder to control a robotic arm by adding a linear Kalman filter based on a kinematic model. Even though this approach demonstrated that a real-time EEG decoding of upper-limb movements is possible, there was a mismatch in the amplitude range between the decoded and actual movements. This amplitude mismatch has been observed in previous works [4], [6], indicating that linear models were not successful in extracting the amplitude or magnitude of the kinematics (e.g., speed in the case of velocity). We recently showed that non-directional (e.g., speed) and directional (e.g., velocity) kinematics are simultaneously encoded in the magnetoencephalogram [11] and EEG [8], and demonstrated that linear models were not able to combine both kinematic signals due to the non-linear relation [8], in contrast to an unscented Kalman filter (UKF) [12].

The purpose of this study was to implement the UKF in an online system to control a robotic arm and assess if it is possible to decode executed upper-limb movements in real-time. In order to alleviate the amplitude mismatch the UKF decoded not only the positions and velocities, but also the instantaneous speed.

II. Materials and Methods

A. Subjects

Five right-handed healthy subjects participated in the study (mean age: 28.2 ± 2.4 years; 2 males, 3 females). The subjects gave their informed written consent and received compensatory payment to participate in the study. The experimental procedure, conforming to the declaration of Helsinki, was approved by the local ethics committee.

B. Experimental setup and paradigm

The experimental setup is depicted in Fig. 1(A). The subject was comfortably seated in front of a screen that depicted a white target trace following a pre-defined trajectory (i.e., "snake"). Three main devices were present: (1) an EEG acquisition system, which monitored the electrical brain activity; (2) a LeapMotion (LM, *LeapMotion Inc., USA*) system, which tracked the position of the user's right hand (visually occluded); and (3) an assistive robotic arm (JACO, *Kinova Robotics Inc., Canada*).

As in [10], the task of the user was to follow the snake's trajectory with the gaze and with the JACO. As shown in Fig. 1(B), JACO was initially controlled by the arm movements captured by the LM. That control was progressively substituted by an EEG-based control up to the point of being completely controlled by an EEG-based decoder at the end of the experiment. The EEG decoder was calibrated with 5 snake runs (100% LM, 0% EEG), and then used in snake runs 6–7 (66% LM, 33% EEG), 8–9 (33% LM, 66%

V. M.-C. and R. H. are with the Biomedical Engineering Group, University of Valladolid, Valladolid, Spain; and with the 'Centro de Investigación Biomédica en Red' in Bioingenieering, Biomaterials and Nanomedicine (CIBER-BBN), Spain (e-mails: victor.martinez@gib.tel.uva.es, robhor@tel.uva.es).

R. J. K., V. M. and G. R. M.-P. are with the Institute of Neural Engineering, Graz University of Technology, Graz, Austria (e-mails: {reinmar.kobler, valeria.mondini, gernot.mueller}@tugraz.at).

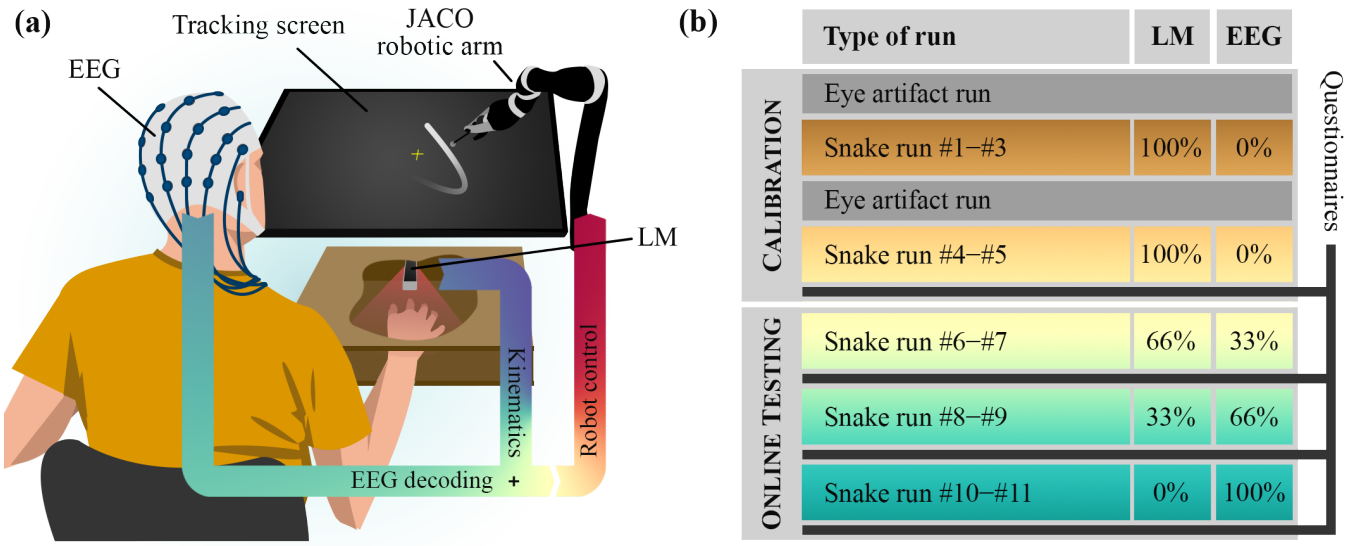

Fig. 1. (a) Experimental setup. The users were seated in front of a screen that depicted a continuous trajectory. The task was to follow the trajectory with the robotic arm (JACO). (b) Paradigm of the study. During calibration, JACO was controlled entirely by the arm movements recorded with a LeapMotion (LM) system. For the feedback runs, the control was reduced until JACO was fully controlled by the EEG.

EEG) and 10–11 (0% LM, 100% EEG). A run typically lasted 5 minutes and was divided into 10 trials. The trials lasted 24 s each and were interleaved with short breaks. Two runs recording eye movements were also performed between calibration blocks. They were used to train an eye artifact correction algorithm according to [13]. After each control condition (100%, 66%, 33% and 0% LM), a questionnaire was fulfilled by the users to collect their impressions.

In order to avoid large movements and consequently motion artifacts, a trial was aborted if the user made movements that were more than 12.5 cm away from the initial position. We additionally decided to map the arm movements to larger movements of JACO; the ratio was 1:2.

The snake's trajectories were generated offline and were the same across users. Twelve of them were generated by sampling band-pass filtered pink noise (0.2–0.4 Hz) [14]. The final set of trajectories was extended by mirroring and rotating (90°, 180° and 270°) this initial set, obtaining a total of 96 different ones. This procedure assured uncorrelated positions and velocities in both horizontal and vertical components [6].

The EEG was recorded using a total of 60 active electrodes (actiCAP, *Brain Products GmbH, Germany*), referenced to the left earlobe and using AFz as ground. Four additional channels were placed at the inferior (left), superior (left) and outer canthi (both) of the eyes to record the electrooculogram as well. All electrodes were connected to biosignal amplifiers (BrainAmp, *Brain Products GmbH, Germany*) with a sampling rate of 500 Hz. Exact locations of the electrodes were initially measured using an ultrasonic positioning system (EPLOS, *Zebris Medical GmbH, Germany*) for each user.

C. Signal processing pipeline

The signal processing pipeline is shown in Fig. 2. In a nutshell, EEG signals were band-pass filtered (0.18–1.5 Hz), spatially filtered (common average reference, CAR) and down-sampled to 20 Hz. The filter specifications were identical to [10]. Pops and drifts were corrected by a high-variance electrode artifact removal (HEAR) algorithm [15]. Eye movements and blinks were corrected with the sparse generalized eye artifact subspace subtraction (SGEYESUB) algorithm [13]. Then, PLS regression projected the EEG data and reduced the dimensionality [5], [8], leading to the final state decoding with a square-root UKF (SQ-UKF) [12]. Meanwhile, the LM signals were low-pass filtered ($<$ 4 Hz) and down-sampled to 20 Hz. The low-pass filter was used to attenuate occasional jitters and measurement noise. Finally, the real and decoded positions were weighted according to the run and scaled (1:2 ratio) to match the movement range of JACO over the screen.

D. EEG decoding of movements

The decoder aimed at estimating the movement state of the user's hand by analyzing the EEG. In particular, we focused on decoding 5 different kinematics: positions p_x and p_y, velocities v_x and v_y and speed $\varsigma = \sqrt{{v_x}^2 + {v_y}^2}$. The latter was added to include information about the amplitude range of the hand trajectories.

PLS regression was used to reduce the co-linearity of the EEG signals and at the same time maintain kinematic information. In detail, we used it to get an initial estimate of the movement states by simultaneously finding the relation between EEG (i.e., $\boldsymbol{E}$) and LM signals, and reducing the dimensionality to $N = 40$ latent components (explaining 70% of variance) [6], [10]. The activity of the latent components is $\hat{\boldsymbol{L}} = \boldsymbol{E}\boldsymbol{W}$; where $\boldsymbol{E} \in \mathbb{R}^{n \times m}$ denotes the calibration period EEG storing previous lags (n samples, $m = 64$ channels $\times$ 7 lags $\in$\{-300 : 50 : 0\} ms), and $\boldsymbol{W} \in \mathbb{R}^{m \times N}$ is the weight matrix. PLS was computed using the SIMPLS algorithm [16]. Afterward, the SQ-UKF, a non-

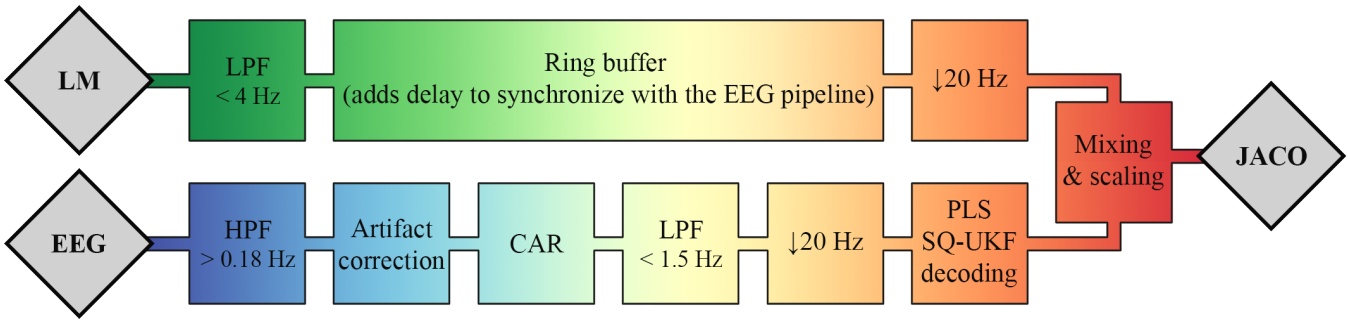

Fig. 2. Online signal processing pipeline followed in this study, in which LM and EEG signals are combined to control the JACO arm.

linear Kalman filter approach, was applied to improve the estimation of the states, assuming that the measurements (i.e., latent component activity) $\hat{\boldsymbol{L}}$ were noisy. As in [8], the SQ-UKF initial parameters were fitted to the calibration data using an encoding approach:

$$\boldsymbol{F} = C_{\boldsymbol{x}_k \boldsymbol{x}_{k-1}} (C_{\boldsymbol{x}_k \boldsymbol{x}_k})^{-1}, \tag{1}$$

$$\boldsymbol{Q} = C_{\boldsymbol{\epsilon}_q \boldsymbol{\epsilon}_q}, \text{ where } \boldsymbol{\epsilon}_q = \boldsymbol{F}\boldsymbol{x}_{k-1} - \boldsymbol{x}_k, \tag{2}$$

$$h(\boldsymbol{x}_k) = C_{\hat{\boldsymbol{l}}_k \boldsymbol{x}_k^+} (C_{\boldsymbol{x}_k^+ \boldsymbol{x}_k^+})^{-1} \cdot \begin{bmatrix} \boldsymbol{x}_k \\ \varsigma(\boldsymbol{x}_k) \end{bmatrix}, \tag{3}$$

$$\boldsymbol{R} = C_{\boldsymbol{\epsilon}_r \boldsymbol{\epsilon}_r}, \text{ where } \boldsymbol{\epsilon}_r = h(\boldsymbol{x}_k) - \hat{\boldsymbol{l}}_k, \tag{4}$$

where $\boldsymbol{F}$ is the state-transition matrix, $\boldsymbol{Q}$ the process noise covariance, $h(\cdot)$ the observation model, $\boldsymbol{R}$ the observation noise covariance, and $C_{\boldsymbol{a},\boldsymbol{b}}$ denotes the covariance matrix between two signals $\boldsymbol{a}$ and $\boldsymbol{b}$. The state at time k is denoted as $\boldsymbol{x}_k = [p_x, v_x, p_y, v_y]_k^T$, becoming $\boldsymbol{x}_k^+ = [\boldsymbol{x}, \varsigma]_k^T$ when speed is included. Note that the non-linearity was included in the measurement equation, whereas the process equation was kept in its linear form. Finally, SQ-UKF returns an estimate of the states $\hat{\boldsymbol{x}}_k$ in real-time, which is further used to control the JACO arm. In the 100% LM condition, we used a cross-validation approach to simulate the EEG decoder on the calibration data (snake runs 1–5).

III. Results

Fig. 3 depicts the main results concerning the quantitative analysis. Correlations between the SQ-UKF decoded $\hat{\boldsymbol{x}}_k$ and the actual LM $\boldsymbol{x}_k$ movement state trajectories are shown for all control conditions, including the upper bound confidence interval of chance level (with significance $\alpha = 0.05$), estimated with a shuffling approach. Moreover, a representative trial is displayed to qualitatively compare the amplitude and shape of LM, PLS and SQ-UKF position trajectories, as well as grand-averaged activation patterns for each kinematic signal. Almost all correlations were above the significance level, except positions and velocities of the Y-axis in the 0% LM condition for some participants. Note that the grand-averaged amplitude ratio between the LM movements and the decoded ones was 1.07 ± 0.09, indicating that the amplitude mismatch was negligible. The trajectories in Fig. 3(B) also show that the amplitudes of the LM and SQ-UKF trajectories were in a similar range, whereas the PLS decoded trajectories indicated a large mismatch in amplitudes.

Qualitative analysis results are depicted in Fig 4. As shown, the users found the task engaging and intuitive, and highlighted that the experiment was neither physically nor mentally demanding. From the questionnaires is also revealed that the users paid more attention to the snake, followed by their own hands, and finally to JACO. As expected, the perceived level of control decreased as the control by LM did. Some users' declared that they felt to be in control of the JACO even in the 100% EEG-based control condition.

IV. Discussion and Conclusion

Correlations between the decoded and recorded LM signals indicate that the online EEG-based decoding of continuous arm movements is feasible. Maximal correlations were reached in the 100% LM condition (p_x: 0.63, v_x: 0.68, p_y: 0.51, v_y: 0.55), which progressively decreased as the fraction of EEG-based decoding increased. Nevertheless, maximal correlations for the 100% EEG control (p_x: 0.39, v_x: 0.48, p_y: 0.35, v_y: 0.44) indicate that movement kinematics can still be decoded in a fully EEG-driven BCI. Since the decoder was fitted to 100% LM condition data and its accuracy was moderate (average correlations of 0.45), the users naturally started to compensate erroneous feedback of the EEG decoder in the shared control conditions. Due to the slight difference in the movement behavior a performance decline was expected. Overall, the correlations are comparable with previous offline results [8], and improved the amplitude mismatch upon the linear Kalman filter based online results [10]. It is also noteworthy that the inclusion of JACO entailed an additional delay between hand and robot movements which, although similar across conditions, was perceived by users as higher as the EEG-based control was.

Owing to the nature of the task; i.e., a low and very limited frequency band, the possibility of observing spurious correlations is real. For that reason, the upper boundary of the chance level correlations (with significance $\alpha = 0.05$) were also calculated. Hence, they serve as a landmark to compare with and assure that the decoding states are not due to chance. Note also that the SQ-UKF works ideally for this kind of task and thus, correlations are expected to decay

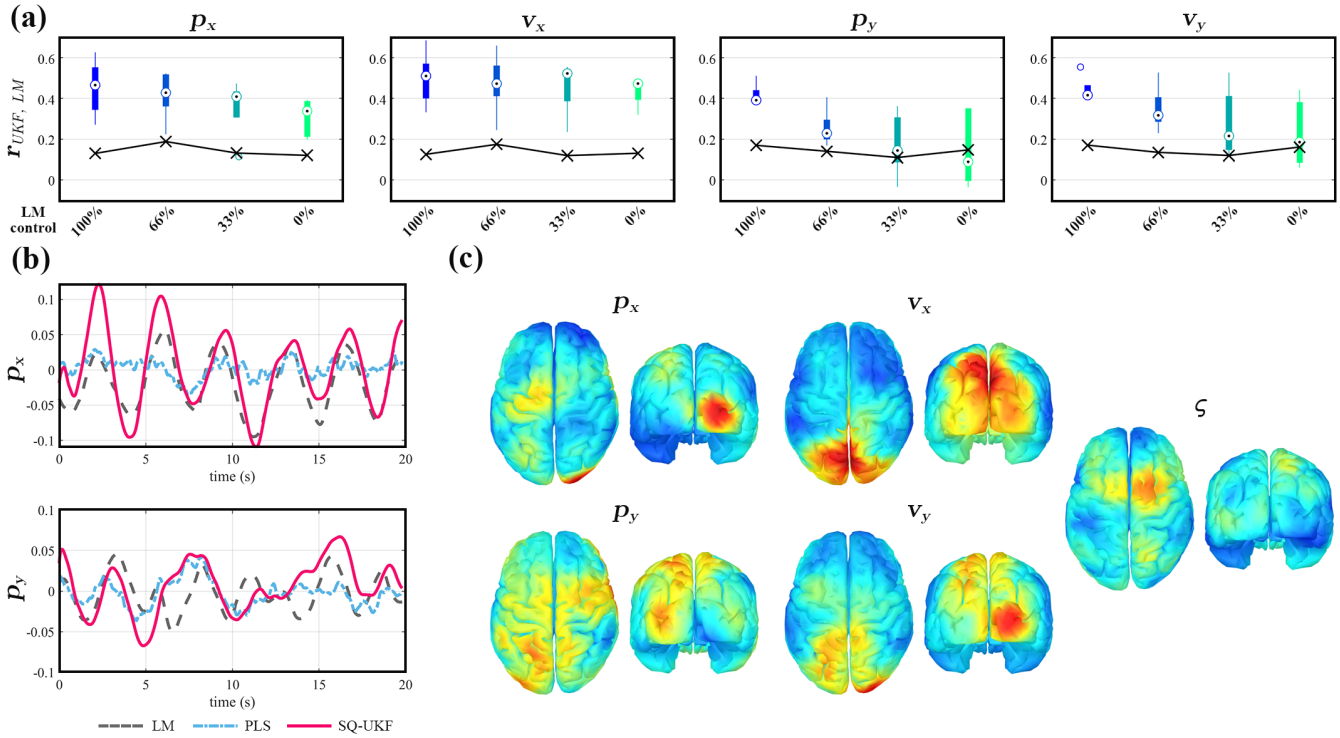

Fig. 3. (a) Feedback runs correlations between the SQ-UKF decoding and the real LM arm movements for each condition and state (chance level is depicted as a black line). (b) Sample trials of 20 s, in which the LM (dashed grey), the PLS decoding (dot-dash blue), and the final SQ-UKF decoding (solid magenta) signals are shown. (c) Averaged activation patterns across subjects in top and back view for each state.

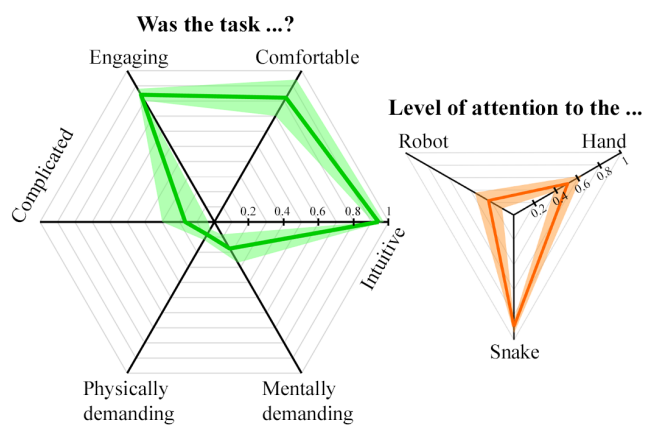

Fig. 4. Normalized questionnaire results regarding (left) the nature of the task and (right) the level of attention users paid to the robot, hand and snake trajectories during the 100% LM condition.

in a "free movement" task, where positions and velocities are not zero-mean or have more variance.

Despite these positive results, we observed that the correlations of the Y-axis kinematics were lower than the X-axis ones. This decrease was especially influential in the 33% and 0% LM condition, leading to correlations near or even at chance level. The rationale could be related to the experimental setup. As shown in Fig. 1(a), the screen was tilted towards the Y-axis to ease the movement of JACO. This leads to a setup in which the perception of vertical movements is ambiguous in comparison with horizontal ones. In other words, to perceive a vertical movement of Δd in Y-axis, JACO needs to move a distance of $d = \Delta d / \sin(\theta)$, where $\theta \sim 45^{\circ}$ is the vertical angle of the screen (i.e., for the X-axis, $d = \Delta d$). This mismatch could influence the perception of the target snake, hindering the encoding of vertical movements. However, further experiments should be carried out in order to determine the actual cause of the phenomenon, since it was not observed in [10]. A decreasing trend of LM signals in 33% and 0% condition trials was also observed, implying that users began to perform movements slightly shifted from the home position. Hence, they lost the initial reference (i.e., origin of coordinates) due to the unawareness of their own hand position when feedback was almost or entirely EEG-based. This behavior could also influence the final decoding.

One of the drawbacks of previous linear studies was that the amplitude of the decoded EEG signals was lower than the actual arm movements [10], causing the users to enlarge their movements to compensate the decoded trajectories. As shown in Fig. 3(b) and [8], this issue has been alleviated by the inclusion of speed in the state space model, leading to an average amplitude ratio of 1.07. Even though speed is linearly encoded in the EEG signals, its relationship with velocities is non-linear. A non-linear approach like the UKF was successful in combining the information and thereby improve the estimation [8].

Concerning the source analysis of the patterns that effectively contributed to the SQ-UKF decoding, we found

activations over the parieto-occipital areas, especially for the velocities. The patterns for positions seem unfocused, with the exception of a demarcate activation on the right occipital lobe only for p_x, which is likely due to a noisy channel. Both results are in accordance with previous studies that associate neural tuning to velocities [6], [10]. As shown in Fig. 3(c), the main activations for speed were over the anterior part of the frontal cortex, close to the primary motor cortex; which can be viewed as a novel result. Note that this observation is slightly different to [8], where speed-related activations peaked in primary sensorimotor cortex. This difference could also be explained by the limited spatial resolution of the source analysis. The resolution was limited since we used a template head model that we co-registered with the users specific electrode locations.

From the questionnaire results, it was clear that the users were satisfied with the task, reporting that they could feel the control of the JACO, even in 33% and 0% LM conditions. Users reported that the task was engaging, intuitive and easy; which were highlighted to be ideal features for BCI training [17] and make users open to participate in further related studies. In general, the strategy of the users was to focus mainly on the snake, putting less attention to their hands or JACO. By focusing on the trajectory, they could ignore possible unexpected shifts in 66%, 33% or 0% conditions due to the decoder, as well as the delay between LM and JACO. In that way, they also avoided performing movements to compensate inaccurate JACO shifts.

The experimental outcomes not only supported that information about upper-limb positions and velocities are encoded in the EEG [6], [8], [10], but also demonstrates that information about speed is present and can be extracted in real-time to improve the position and velocity decoder accuracy. In conclusion, a non-linear decoder based on SQ-UKF has been proved to be suitable for decoding user movements from non-invasive recordings in real-time, providing moderate correlations.

In spite of these encouraging results, several limitations were identified. Firstly, the users were not aware of their own upper-limb positions when EEG decoding gained importance, leading to shifts from the home position that may influence the final decoding. This issue could be addressed by depicting a pointer that indicates the current LM position on the screen. Secondly, the Y-axis decoding yielded lower correlations than X-axis. Further work is required to investigate the reason and adapt the setup to overcome this limitation. Lastly, the number of users that participated in the study was limited (5 participants). An additional effort to recruit more participants, or even motor-disabled users, is necessary to generalize these results.

V. Acknowledgments

This study has received funding from the European Research Council (ERC) under the European Union's Horizon 2020 programme (Consolidation Grant 681231 'Feel Your Reach') and from the CIBER-BBN through 'Instituto de Salud Carlos III' and 'European Regional Development Fund' (FEDER), as well as from projects 'DPI2017-84280-R' of 'Ministerio de Ciencia, Innovación y Universidades' and FEDER, and the project '0378_AD_EEGWA_2_P' (Interregional cooperation program VA Spain-Portugal POCTEP 2014-2020) of the European Commission and FEDER. V. Martínez-Cagigal was in receipt of a PIF UVa grant from the University of Valladolid.

References

[1] G. R. Müller-Putz, A. Schwarz, J. Pereira *et al.*, "From classic motor imagery to complex movement intention decoding: The noninvasive Graz-BCI approach," in *Progress in Brain Research*. Elesvier, 2016, vol. 228, pp. 39–70, iSSN: 18757855.

[2] L. R. Hochberg, D. Bacher, B. Jarosiewicz *et al.*, "Reach and grasp by people with tetraplegia using a neurally controlled robotic arm," *Nature*, vol. 485, no. 7398, pp. 372–375, 2012.

[3] T. J. Bradberry, R. J. Gentili, and J. L. Contreras-Vidal, "Reconstructing three-dimensional hand movements from noninvasive electroencephalographic signals," *J.Neurosci.*, vol. 30, no. 9, 2010.

[4] J. M. Antelis, L. Montesano, A. Ramos-Murguialday *et al.*, "On the Usage of Linear Regression Models to Reconstruct Limb Kinematics from Low Frequency EEG Signals," *PLoS ONE*, vol. 8, no. 4, 2013.

[5] P. Ofner and G. R. Müller-Putz, "Using a noninvasive decoding method to classify rhythmic movement imaginations of the arm in two planes," *IEEE TBME*, vol. 62, no. 3, pp. 972–981, 2015.

[6] R. J. Kobler, A. I. Sburlea, and G. R. Müller-Putz, "Tuning characteristics of low-frequency EEG to positions and velocities in visuomotor and oculomotor tracking tasks," *Sci. Rep.*, vol. 8, pp. 1–14, 2018.

[7] A. Korik, R. Sosnik, N. Siddique *et al.*, "Decoding Imagined 3D Hand Movement Trajectories From EEG: Evidence to Support the Use of Mu, Beta, and Low Gamma Oscillations," *Frontiers in Neuroscience*, vol. 12, no. March, pp. 1–16, 2018.

[8] R. J. Kobler, A. I. Sburlea, V. Mondini *et al.*, "Distance and speed informed kinematics decoding improves M/EEG based upper-limb movement decoder accuracy," *J. Neural Eng.*, in review.

[9] J. Lv, Y. Li, and Z. Gu, "Decoding hand movement velocity from electroencephalogram signals during a drawing task." *Biomedical engineering online*, vol. 9, no. 1, 2010, iSBN: 1475-925X.

[10] V. Mondini, R. J. Kobler, A. I. Sburlea *et al.*, "Continuous low-frequency EEG decoding of arm movement for closed-loop, natural control of a robotic arm," submitted.

[11] R. J. Kobler, M. Hirata, H. Hashimoto *et al.*, "Simultaneous decoding of velocity and speed during executed and observed tracking movements: an MEG study," in *Proc. of the 8th Graz BCI Conference 2019*, Graz, 2019.

[12] R. Van der Merwe and E. Wan, "The square-root unscented Kalman filter for state and parameter-estimation," in *Proc. of the IEEE ICASP*, 2001.

[13] R. J. Kobler, A. I. Sburlea, C. Lopes-Dias *et al.*, "Corneo-retinal-dipole and eyelid-related eye artifacts can be corrected offline and online in electroencephalographic and magnetoencephalographic signals," *NeuroImage*, in revision.

[14] L. Paninski, M. R. Fellows, N. G. Hatsopoulos *et al.*, "Spatiotemporal Tuning of Motor Cortical Neurons for Hand Position and Velocity," *Journal of Neurophysiology*, vol. 91, no. 1, pp. 515–532, 2004.

[15] R. J. Kobler, A. I. Sburlea, V. Mondini *et al.*, "HEAR to remove pops and drifts: the high-variance electrode artifact removal (HEAR) algorithm," in *Proc. of the IEEE EMBC*, Jul. 2019.

[16] S. de Jong, "SIMPLS: an alternative approach to partial least squares regression," *Chemom. Intell. Lab. Syst.*, vol. 18, no. 3, 1993.

[17] F. Lotte and C. Jeunet, "Towards improved bci based on human learning principles," in *The 3rd International Winter Conference on Brain-Computer Interface*. IEEE, 2015, pp. 1–4.